

Nonvanishing optimal noise in cellular automaton model of self-propelled particles

Guang-Le Du(杜光乐) and Fang-Fu Ye(叶方富)

Citation: Chin. Phys. B, 2022, 31 (**8**): 086401. DOI: 10.1088/1674-1056/ac67c4
Journal homepage: http://cpb.iphy.ac.cn; http://iopscience.iop.org/cpb

What follows is a list of articles you may be interested in

Doping effects on the stacking fault energies of the γ' phase in Ni-based superalloys

Weijie Li(李伟节), Chongyu Wang(王崇愚)
Chin. Phys. B, 2020, 29 (**2**): 026401. DOI: 10.1088/1674-1056/ab6203

Variational and diffusion Monte Carlo simulations of a hydrogen molecular ion in a spherical box

Xuehui Xiao(肖学会), Kuo Bao(包括), Youchun Wang(王友春), Hui Xie(谢慧), Defang Duan(段德芳), Fubo Tian(田夫波), Tian Cui(崔田)
Chin. Phys. B, 2019, 28 (**5**): 056401. DOI: 10.1088/1674-1056/28/5/056401

The affection on the nature of percolation by concentration of pentagon-heptagon defects in graphene lattice

Yuming Yang(杨宇明), Baohua Teng(滕保华)
Chin. Phys. B, 2018, 27 (**10**): 106401. DOI: 10.1088/1674-1056/27/10/106401

Effects of the trimodal random field on the magnetic properties of a spin-1 Ising nanotube

H. Magoussi, A. Zaim, M. Kerouad
Chin. Phys. B, 2013, 22 (**11**): 116401. DOI: 10.1088/1674-1056/22/11/116401

Simulations of the flipping images and microparameters of molecular orientations in liquids according to molecule string model

Wang Li-Na, Zhao Xing-Yu, Zhang Li-Li, Huang Yi-Neng
Chin. Phys. B, 2012, 21 (**8**): 086403. DOI: 10.1088/1674-1056/21/8/086403

Nonvanishing optimal noise in cellular automaton model of self-propelled particles

Guang-Le Du(杜光乐)[1] and Fang-Fu Ye(叶方富)[1,2,†]

[1] *Beijing National Laboratory for Condensed Matter Physics, Institute of Physics, Chinese Academy of Sciences, Beijing* 100190, *China*
[2] *School of Physical Sciences, University of Chinese Academy of Sciences, Beijing* 100049, *China*

(Received 26 March 2022; accepted manuscript online 18 April 2022)

A minimal cellular automaton model is introduced to describe the collective motion of self-propelled particles on two-dimensional square lattice. The model features discretization of directional and positional spaces and single-particle occupation on one lattice site. Contrary to the Vicsek model and its variants, our model exhibits the nonvanishing optimal noise. When the particle density increases, the collective motion is promoted with optimal noise strength and reduced with noise strength out of optimal region. In addition, when the square lattice undergoes edge percolation process, no abrupt change of alignment behaviors is observed at the critical point of percolation.

Keywords: self-propelled particle, optimal noise, cellular automaton

PACS: 64.60.Cn, 64.60.De, 64.60.aq **DOI:** 10.1088/1674-1056/ac67c4

1. Introduction

Collective motion, as a ubiquitous phenomenon spanning different spatio-temporal scales, is observed in live systems such as human beings[1] and animals,[2,3] bacteria[4,5] and cells,[6] and also in systems consisting of artificial devices.[7] Self-propelled particles (SPPs) subject to both alignment interaction and noises can undergo a phase transition from disordered to ordered collective motion by decreasing noise or increasing particle density.[8,9] A long-range alignment order parameter can be used to characterize the continuous spontaneous symmetry breaking accompanying the phase transition. Vicsek model,[8] a minimal model to depict the phase transition, has been extended in various aspects since its appearance, such as from polar to apolar particles,[10,11] from intrinsic scalar noise to vectorial noise,[9] and extensions of interactions to include, e.g., cohesion[12] and disordered environments.[14,15] One particular kind of variants is to change the space where SSPs reside from two-dimensional Euclidean space to lattices[16,17] or general manifolds[18] and/or from continuous directional space to discrete ones.[19,20]

In Vicsek model and its variants, it is long accepted that the collective motion is optimized with vanishing noise and maximal particle density.[8,9,21] Surprisingly, in Refs. [22,23] it is found that when SSPs move in heterogeneous media or contrarian particles are added, the optimal collective motion is achieved with nonvanishing noise. Here we introduce a minimal cellular automaton model on square lattice that also exhibits nonvanishing optimal noise. Compared to previous models,[22,23] our model includes no complicated interactions and features discretization of directional and positional spaces and single-particle occupation on one lattice site. The nonvanishing optimal noise results from the blocked motion in the discrete spaces. It is also noteworthy that when noise strength deviates from optimal regime, the collective motion is reduced by increasing particle density. The square lattice is further subjected to edge percolation process to mimic the environmental disorder. No noticeable abrupt impact of the underlying percolation on the collective motion is observed at the critical point of percolation.

2. Cellular automaton model

In order to investigate the collective motion of self-propelled particles in discrete space, we here introduce a cellular automaton model on two-dimensional square lattice, possibly undergoing edge percolation process. The model bears two defining features: i) positional and directional spaces are discrete; and ii) one lattice site can be occupied by at most one particle. One of the immediate consequences of these two defining features is that the motion of SSPs can be blocked with high probability, which is, in contrast, a rare event in Vicsek model with both positional and directional spaces being continuous. Nonvanishing noise can promote the collective motion by helping merge the clusters blocking the motion of each other. In order to mimic the environmental disorder, the lattice is further subjected to edge percolation process with edge occurrence probability p. Attention is focused on the behaviors of collective motion at the critical point of percolation.

We now introduce how the directions and positions of particles are updated in the model. As illustrated in Fig. 1, the direction of a particle is in the discrete set $\mathcal{D} = \{(-1,0),(1,0),(0,1),(0,-1)\}$, representing, respec-

†Corresponding author. E-mail: fye@iphy.ac.cn

© 2022 Chinese Physical Society and IOP Publishing Ltd

tively, left, right, up and down directions. Denote the direction of i-th particle at time t_k as $\boldsymbol{d}_i(t_k) \in \mathcal{D}$ and vectorial noise $\boldsymbol{\eta}_i(t_k) \in \eta\mathcal{D}$ with η being the noise strength. The directions of all particles are updated synchronously as follows. Firstly, at time t_k, we calculate $\boldsymbol{d}_i^{\rm tot}(t_k) = \sum_{j\sim i} \boldsymbol{d}_j(t_k) + \boldsymbol{\eta}_i(t_k)$, where $\sum_{j\sim i}$ means summation over i-th particle and all its neighboring particles. If the lattice undergoes edge percolation process, only particles with an edge connecting each other are considered neighbors. Next, we calculate the polar angle of $\boldsymbol{d}_i^{\rm tot}(t_k)$, $\theta_i(t_k) = \text{atan2}(d_{i,y}^{\rm tot}, d_{i,x}^{\rm tot})$, where atan2 is 2-argument arctangent returning values in the range $(-\pi, \pi]$ and $d_{i,x}^{\rm tot}$ and $d_{i,y}^{\rm tot}$ are, respectively, the x and y components of $\boldsymbol{d}_i^{\rm tot}$. The direction of i-particle at time t_{k+1} is

$$\boldsymbol{d}_i(t_{k+1}) = \begin{cases} (1,0), & \theta_i(t_k) \in \left(-\dfrac{\pi}{4}, \dfrac{\pi}{4}\right), \\ (0,1), & \theta_i(t_k) \in \left(\dfrac{\pi}{4}, \dfrac{3\pi}{4}\right), \\ (0,-1), & \theta_i(t_k) \in \left(-\dfrac{3\pi}{4}, -\dfrac{\pi}{4}\right), \\ (-1,0), & \theta_i(t_k) \in \left(-\pi, -\dfrac{3\pi}{4}\right) \cup \left(\dfrac{3\pi}{4}, \pi\right], \\ \boldsymbol{d}_i(t_k), & \text{otherwise.} \end{cases} \tag{1}$$

The reason for a particle maintaining its original direction when $\theta_i(t_k)$ equals to $\pm\pi/4$ or $\pm 3\pi/4$ is that we here mainly consider macroscopic entities such as vehicles or pedestrians, where thermal fluctuations are negligible. In this case, maintaining the original direction is the most natural choice. Next, the positions of particles are updated asynchronously by traversing all particles row after row. Denote the position of i-th particle at time t_k as $\boldsymbol{r}_i(t_k)$. The position at time t_{k+1} is proposed to be

$$\boldsymbol{r}_i(t_{k+1}) = \boldsymbol{r}_i(t_k) + \boldsymbol{d}_i(t_{k+1}). \tag{2}$$

If the position $\boldsymbol{r}_i(t_{k+1})$ is connected to $\boldsymbol{r}_i(t_k)$ by a lattice edge and not occupied by other particles yet, then the proposal is accepted; otherwise, the proposal is rejected and $\boldsymbol{r}_i(t_{k+1}) = \boldsymbol{r}_i(t_k)$.

We now define the order parameters to be investigated in present study. Assume there are n particles and N lattice sites. The particle density is then $\rho = n/N$. The global alignment order parameter is defined in the same way as that in Vicsek model

$$\phi = \frac{1}{n}\left|\sum_i \boldsymbol{d}_i^{\rm st}\right|, \tag{3}$$

where $\boldsymbol{d}_i^{\rm st}$ is the direction of i-th particle in steady state, the summation $\sum_i$ traverses all particles, and $|\cdot|$ is the norm of a vector. ϕ cannot capture the information of local alignment structures. The discretization of both directional and positional spaces enables us to define alignment cluster, i.e., the maximal set of particles with the same direction fulfilling the condition that positions of any two particles in the set are connected by a lattice edge. We define the normalized maximal size of all alignment clusters as an additional order parameter

$$S = \frac{1}{n}\max\{S_1, S_2, \ldots, S_i, \ldots\}, \tag{4}$$

where S_i is the size of the i-th alignment cluster.

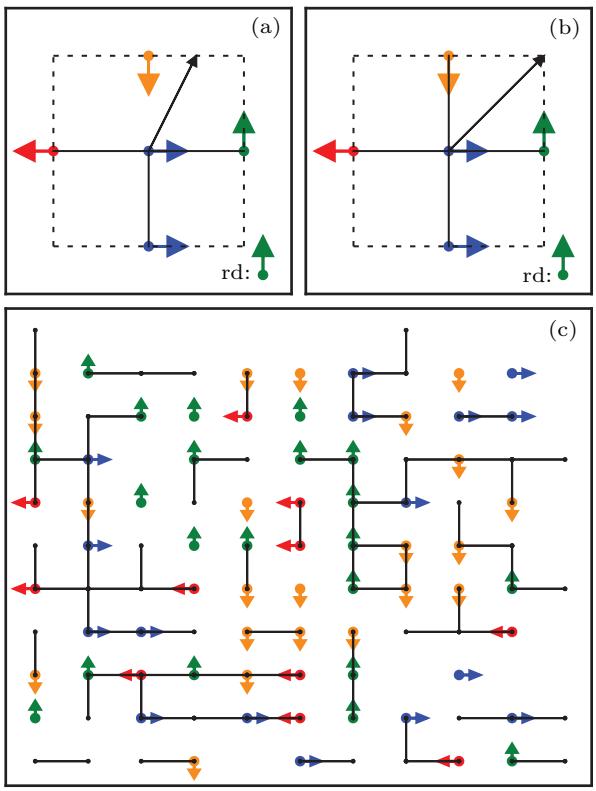


Fig. 1. Schematic illustration of how the directions of particles update. In panels (a) and (b), vectorial noises are label by "rd" and their strengths are both $\eta = 1$. The black arrows represent $\boldsymbol{d}^{\rm tot}$ scaled. (a) Direction of the central particle at next time step is up since $\theta \in (\pi/4, 3\pi/4)$. Note the direction of down particle is not counted, since it is not connected to the central particle. (b) With $\theta = \pi/4$, the particle at next time step maintains its current right direction. (c) Typical configuration when the lattice undergoes edge percolation with edge occurrence probability 0.36.

The simulation is conducted as follows. The system size is 100×100 and the periodic boundary condition is applied. In order to investigate how particle density ρ and noise strength η affect the collective motion, ρ and η are fixed in each realization of simulation and varied across different realizations with ranges $\rho \in [0.1, 1]$ and $\eta \in [0, 4]$. The initial positions and directions of particles are generated randomly from the allowed spaces and follow the single-particle occupation rule. Then the directions and positions are updated following the rules introduced above. We make sure the system has already reached steady state by evolving the system for 500 time steps. Then the two order parameters at steady state are calculated. To reduce the influence of fluctuations at steady state, we take the average of the order parameters over the last 100 time steps. All the data of the order parameters ϕ and S are obtained by taking average over 100 realizations with different

initial configurations. The simulation is firstly performed with the underlying lattice undergoing no edge percolation and being fully-connected. Then the simulation is repeated but with edge percolation turned on.

3. Results and discussion

We first present the results without edge percolation applied on the underlying lattice. In Fig. 2, two order parameters ϕ and S versus noise strength η and particle density ρ are shown. From Figs. 2(a) and 2(b), one can see clearly that there are a range of noise strengths, approximately $[1.5, 3]$ that maximizes the two alignment order parameters with varying particle densities. Hence the optimal noise for the collective motion is nonvanishing in our model. This is due to the fact that moderate noise strength can promote the merge of alignment clusters. Too large noise strength will, however, destabilise alignment clusters. These two competing effects result in intermediate noise strength such that the collective motion is optimal. Thus we may divide noise strengths into two regimes, optimal and nonoptimal regimes. It is noteworthy that in the nonoptimal regime, large noise strength leads to lower ϕ and S than small noise strength, indicating that large noise fluctuations are more efficient to suppress the collective motion than blocking motion of alignment clusters.

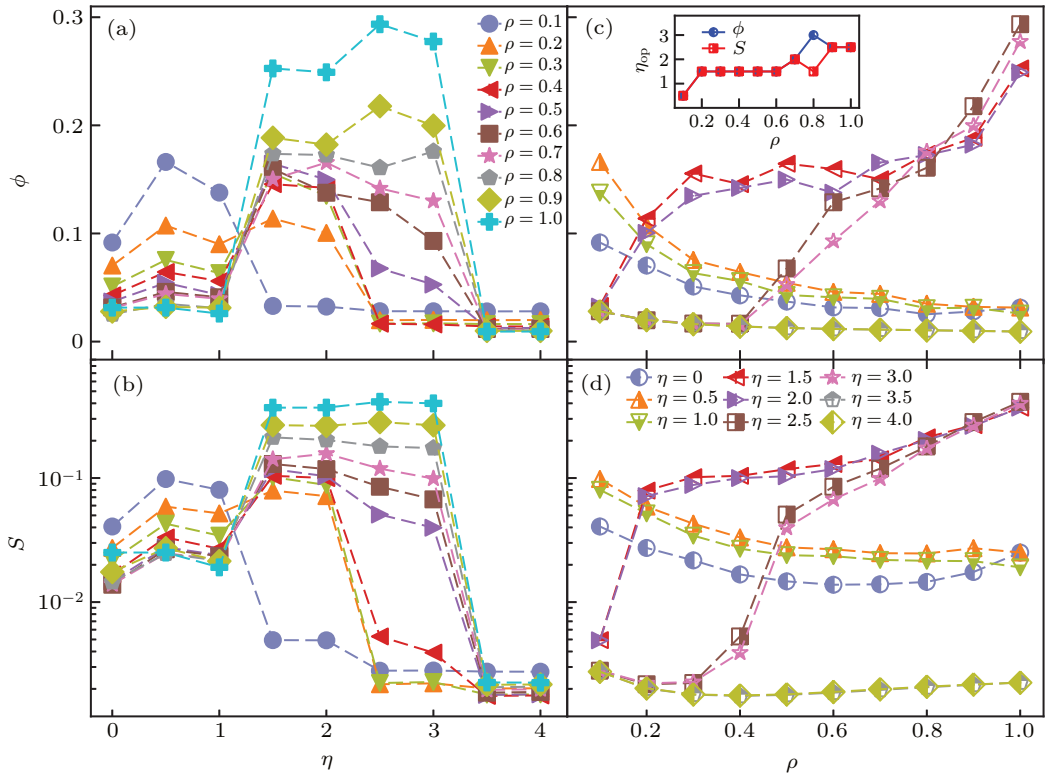


Fig. 2. Order parameters ϕ and S versus noise strength η with different particle densities (a), (b) and versus particle density with different noise strengths (c), (d) when there is no edge percolation on the underlying lattice. In the inset of panel (c) is the optimal noise strength that maximizes, respectively, ϕ and S for fixed particle density ρ. The legend in panel (b) is the same as that in panel (a). The legend in panel (c) is the same as that in panel (d).

In Figs. 2(c) and 2(d), one can observe very different behaviors of ϕ and S when ρ varies with noise strengths in the two regimes. For noise strength in the optimal regime, both ϕ and S increase with increasing ρ. For noise strength in the nonoptimal regime, ϕ constantly decreases with increasing ρ; there is optimal ρ for S at extremely small or large noise strengths. In the inset of Fig. 2(c), the optimal noise strengths that maximize respectively, and ϕ and S are shown to be increasing with increasing ρ, which indicates higher particle density entails larger noise fluctuations to merge alignment clusters most efficiently.

In Fig. 3, we show some typical configurations at steady state with different particle densities and noise strengths. In Figs. 3(a) and 3(b), the particle densities are all $\rho = 0.3$ and noise strengths are, respectively, $\eta = 1$ and $\eta = 2$. In Figs. 3(c) and 3(d), the particle densities are all $\rho = 0.9$ and noise strengths are, respectively, $\eta = 1$ and $\eta = 2$. One can clearly see when the noise strength is small ($\eta = 1$ away from optimal regime), the sizes of alignment clusters are relatively small. When noise strength increases to optimal regime ($\eta = 2$), the alignment clusters are merged into larger clusters, which promotes the collective motion. Even larger noise strengths will destabilise alignment clusters and randomize the directions of individual particles, and consequently reduce the overall collective motion. So it is moderate noise strength that optimizes the collective motion. When noise strength is in

the optimal regime, increasing particle density leads to higher contact probability of alignment clusters that will merge with optimal noise strengths. When noise strength is out of the optimal regime, the increase of particle density causes more blocking of motion irresolvable by small noise strength, promotes the destabilisation of alignment clusters by too large noise strength, and consequently reduces the collective motion. We thus complete explaining qualitatively the behaviors with noise strengths in both optimal and nonoptimal regimes observed in Fig. 2 by comparing different configurations in steady state.

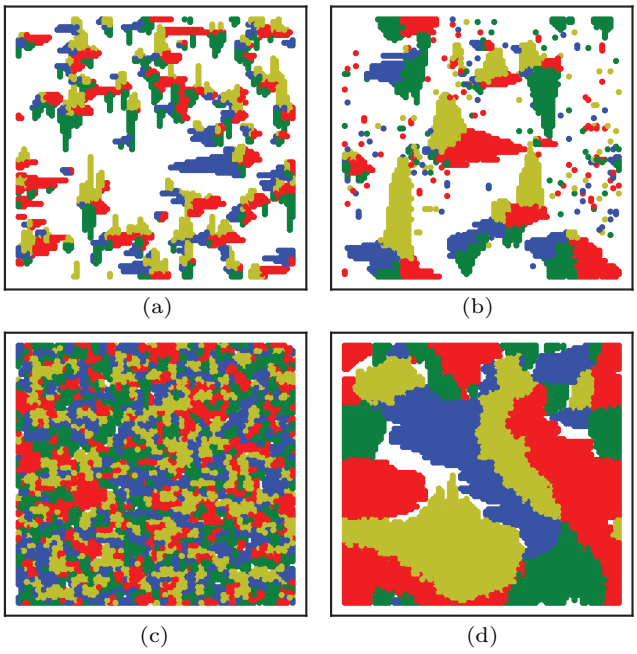


Fig. 3. Typical configurations at steady state with different noise strengths and particle densities when there is no edge percolation on the underlying lattice. In panels (a) and (b), the particle densities are all $\rho = 0.3$ and noise strengths are, respectively, $\eta = 1$ and $\eta = 2$. In panels (c) and (d), the particle densities are all $\rho = 0.9$ and noise strengths are, respectively, $\eta = 1$ and $\eta = 2$. The directions right, left, up and down are coded by, respectively, blue, red, green and orange colors.

It is noteworthy that in Fig. 3, the blocking of particle motion bears some resemblances of jamming in, e.g., granular materials. When particle density is increased, the probability of motion being blocked increases. The increase of noise strength, acting the role of temperature, can make clusters unjam by merging them into mobile ones. Corresponding to force chains found in jammed granular systems,[13] the most probable configurations, as one can observe from Fig. 3, follow a contact pattern where horizontal and vertical directions alternate. However, there is no pressure concept in our model. The blocking of motion can happen even for very sparse systems due to the discretization of directional and positional spaces. Traffic jams, as a particular kind of jamming where active agents are jammed, can be described by Nagel–Schreckenberg model.[25] Our model, being also of cellular automaton type, differs from Nagel–Schreckenberg model in model settings and other relevant levels.

In order to mimic environmental disorder, the lattice is further subjected to edge percolation process. Percolating networks have been used to study swarming phase transition.[14] Two-layer or multilayer networks have been used to study, for example, epidemic or information propagation in social networks.[24] In our model, the percolating lattice and alignment clusters combined constitute a two-layer network. Our main motivation to apply percolating lattice is to observe its impact on the collective motion of SSPs at the critical point of percolation. Intuitively, the abrupt increase of cluster size in the underlying lattice may have large impact on the alignment behaviors of particles, since the motion of particles is confined by the percolating lattice.

Figure 4 shows order parameters ϕ and S versus edge occurrence probability p with different noise strengths and particle densities when the underlying lattice undergoes edge percolation process. Note on infinite square lattice, the critical point of edge percolation is $p_c = 0.5$ and on finite square lattice p_c is slightly less than 0.5. From Fig. 4, one can observe no noticeable abrupt change of the alignment behaviors at the critical point of percolation. Although adding small number of edges leads to the emergence of a giant percolating cluster in the underlying lattice, it only affects the overall alignment behaviors continuously instead of abruptly. Both ϕ and S increase with increasing p because less confined motion promotes merge of alignment clusters.

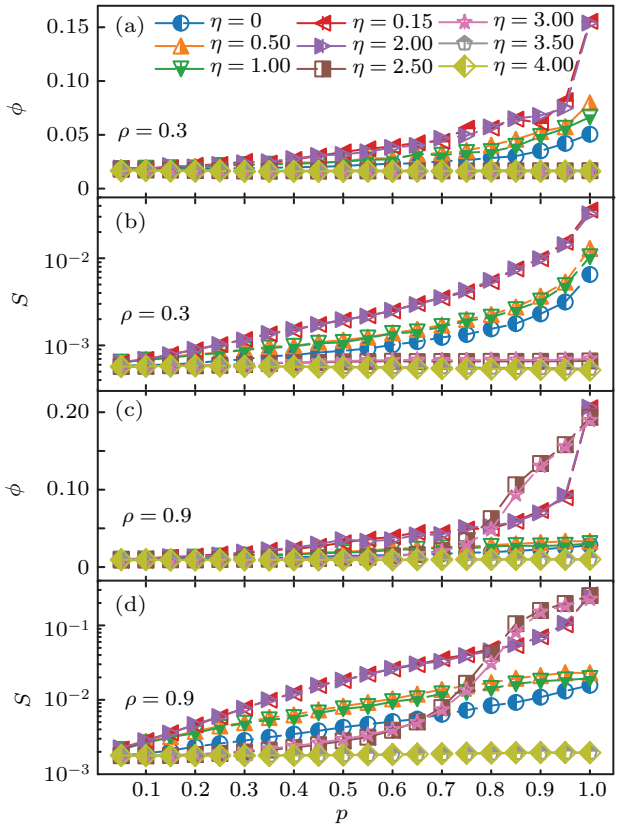


Fig. 4. Order parameters ϕ and S versus edge occurrence probability p with different noise strengths and particle densities when the underlying lattice is subjected to edge percolation. Legends in panels (b)–(d) are the same as that in panel (a).

4. Conclusion

In conclusion, we construct a minimal cellular automaton model to describe the collective motion of self-propelled particles on two-dimensional square lattice. The discretization of directional and positional spaces enables the definition of alignment clusters. Max size of alignment clusters along with average of directions is introduced as an additional order parameter to characterise local as well as global alignment structures. Nonvanishing noise optimizing the collective motion is observed. In the optimal regime of noise strengths, the collective motion is promoted by increasing particle density. This can be accounted for by that moderate noise strength can help merge of alignment clusters without destabilising them. In the nonoptimal regime of noise strengths, the collective motion is, however, reduced by increasing particle density. This is because high particle density increases the probability of blocked motion irresolvable by small noise strength and promotes the destabilisation of alignment clusters by too large noise strength. When the underlying lattice undergoes edge percolation process, no abrupt change of alignment behaviors is observed at the critical point of percolation. The edge percolation has only continuous effects on the alignment behaviors of particles over the whole range of edge occurrence probabilities. Our model can help understand the collective motion of particles in discrete spaces and has potential applications in alleviating traffic jams.[16,17,25–27]

Acknowledgements

Project supported by the Strategic Priority Research Program of Chinese Academy of Sciences (Grant No. XDB33000000) and the National Natural Science Foundation of China (Grant No. 12090054).

References

[1] Helbing D, Farkas I and Vicsek T 2000 *Nature* **407** 487
[2] Cavagna A, Cimarelli A, Giardina I, Parisi G, San-tagati R, Stefanini F and Viale M 2010 *Proc. Natl. Acad. Sci. USA* **107** 11865
[3] Bhattacharya K and Vicsek T 2010 *New J. Phys.* **12** 093019
[4] Zhang H P, Béer A, Florin E L and Swinney H L 2010 *Proc. Natl. Acad. Sci. USA* **107** 13626
[5] Dombrowski C, Cisneros L, Chatkaew S, Goldstein R E and Kessler J O 2004 *Phys. Rev. Lett.* **93** 098103
[6] Riedel I H, Kruse K and Howard J 2005 *Science* **309** 300
[7] Takagi D, Palacci J, Braunschweig A B, Shelley M J and J Zhang 2014 *Soft Matter* **10** 1784
[8] Vicsek T, Czirók A, Ben-Jacob E, Cohen I and Shochet O 1995 *Phys. Rev. Lett.* **75** 1226
[9] Grégoire G and Chaté H 2004 *Phys. Rev. Lett.* **92** 025702
[10] Chaté H, Ginelli F and Montagne R 2006 *Phys. Rev. Lett.* **96** 180602
[11] Narayan V, Ramaswamy S and Menon N 2007 *Science* **317** 105
[12] Grégoire G, Chaté H and Tu Y 2003 *Phys. D* **181** 157
[13] Cates M E, Wittmer J P, Bouchaud J P and Claudinet P 1998 *Phys. Rev. Lett.* **81** 1841
[14] Quint D A and Gopinathan A 2015 *Phys. Biol.* **12** 046008
[15] Morin A, Desreumaux N, Caussin J B and Bartolo D 2016 *Nat. Phys.* **13** 63
[16] Peruani F, Klauss T, Deutsch A and Voss-Boehme A 2011 *Phys. Rev. Lett.* **106** 128101
[17] Csahok Z and T Vicsek 1994 *J. Phys. Math. Gen.* **27** L591
[18] Li W 2015 *Sci. Rep.* **5** 13603
[19] Bussemaker H J, Deutsch A and Geigant E 1997 *Phys. Rev. Lett.* **78** 5018
[20] Csahók Z and Vicsek T 1995 *Phys. Rev. E* **52** 5297
[21] Chaté H, Ginelli F, Grégoire G and Raynaud F 2008 *Phys. Rev. E* **77** 046113
[22] Chepizhko O, Altmann E G and Peruani F 2013 *Phys. Rev. Lett.* **110** 238101
[23] Bonilla L L and Trenado C 2019 *Phys. Rev. E* **99** 012612
[24] Boccaletti S, Bianconi G, Criado R, del Genio C I, Gómez-Gardeñes J, Romance M, Sendiña-Nadal I, Wang Z and Zanin M 2014 *Phys. Rep.* **544** 1
[25] Nagel K and Schreckenberg M 1992 *J. Phys. I France* **2** 2221
[26] Li Z, Liu F and Sun J 2011 *Chin. Phys. B* **20** 088901
[27] Lefauve A and Saintillan D 2014 *Phys. Rev. E* **89** 021002